J Mol Model (2013) 19:2383–2389
DOI 10.1007/s00894-013-1788-x

ORIGINAL PAPER

Theoretical study about the 5-azido-1H-tetrazole and its ion salts

Kun Wang · Jianguo Zhang · Jing Shang · Tonglai Zhang

Received: 19 October 2012 / Accepted: 28 January 2013 / Published online: 15 February 2013

Abstract Periodic DFT method has been firstly used to calculate the bulk structure, electronic structure, electrical transferring and thermodynamic properties of crystalline 5-azido-1H-tetrazole (HCN_7) and its four different salts. The anion CN_7^- was included in all of the salts such as ammonium 5-azidotetrazolate ($[NH_4]^+[CN_7]^-$), hydrazinium 5-azidotetrazolate ($[N_2H_5]^+[CN_7]^-$), guanidinium 5-azidotetrazolate ($[CH_6N_3]^+[CN_7]^-\cdot H_2O$) and 1-aminoguanidinium 5- azidotetrazolate ($[CH_7N_4]^+[CN_7]^-$). The simulation is in reasonable agreement with the experimental results. It is found the salts of HCN_7 are more stable than itself because the band gap of the salts is larger. The density of state shows the *p* states of them (including HCN_7 and its four salts) have played a very significant role in the reaction.

Keywords Azidotetrazole · Density of state · DFT calculation · Nitrogen heterocycles

Introduction

Since 1893 people have studied tetrazole for its sensational stabilities in nitrogen heterocyclic compounds [1]. Then its energetic properties were found to be appropriate for the utilization as the propellants and explosives [2]. The jobs were summarized by Morison last century [3]. Taylor put the hypothesis of 5-azido-1H-tetrazole into reality [4]. The utilization safety of energetic tetrazole has been studied in Sandia National Laboratory for many years [5], but it still attracts many scientists to increase the content of nitrogen to improve the explosive properties of the series of energetic materials. Especially the successful synthesis of 2-(5-cyanotetrazole) pentammine cobalt (III) perchlorate, (CP explosive for short), attracted much attention [6–8]. Subsequently, some energetic groups such as nitryl, amino especially the azido [9–13] and different metal cations have been introduced into the original molecule, that indeed improve the explosive properties [14–17]. Stierstorfer first synthesized 5-azido-1H-tetrazole (HCN_7) and proved it can form an anion by losing one hydrogen ion [17]. Gerhard and Hammerl studied some energetic dihydrazinium salt such as $[N_2H_5]^+{}_2[N_4C\text{-}N{=}N\text{-}CN_4]^{2-}$ [14], at the same time, the methods of synthesis HCN_7, $PhCN_7$ and HCN_9 were also pointed out [16].

With the properties of the high nitrogen content as well as the high enthalpy of formation, certainly HCN_7 has been paid special attention in many countries [9, 13, 17–19]. Here we studied the relative properties of HCN_7 as a crystalline and the derivative salts containing CN_7^- with DFT method.

5-azido-1H-tetrazole (HCN_7, for convenience, this compound will be called **A** in this paper) [17] consists of eight molecules in a monoclinic unit cell, with a $P2_1/c$ space group. The structure of the ammonium 5-azdiotetrazolate ($[NH_4]^+[CN_7]^-$, **B** for convenience) is similar with **A**, while only two repeating units are in the cell. Hydrazinium 5-azidotetrazolate ($[N_2H_5]^+[CN_7]^-$, **C** for convenience) and guanidinium 5-zaidotetrazolate ($[CH_6N_3]^+[CN_7]^-\cdot H_2O$, **D** for convenience) are monoclinic crystals with $P2_1/c$ spaces, both containing four molecuar anions in their unit cells respectively. And the unit cell of 1-amino-guanidinium 5-azdiotetrazolate ($[CH_7N_4]^+[CN_7]^-$, **E** for convenience) triclinic with $P\overline{1}$ space group. Two repeating molecules are in the unit cells. The crystal structures of the five compounds are displayed in Fig. 1(I).

K. Wang · J. Zhang (✉) · J. Shang · T. Zhang
State Key Laboratory of Explosion Science and Technology, Beijing Institute of Technology, Beijing 100081, People's Republic of China
e-mail: zhangjianguobit@yahoo.com.cn

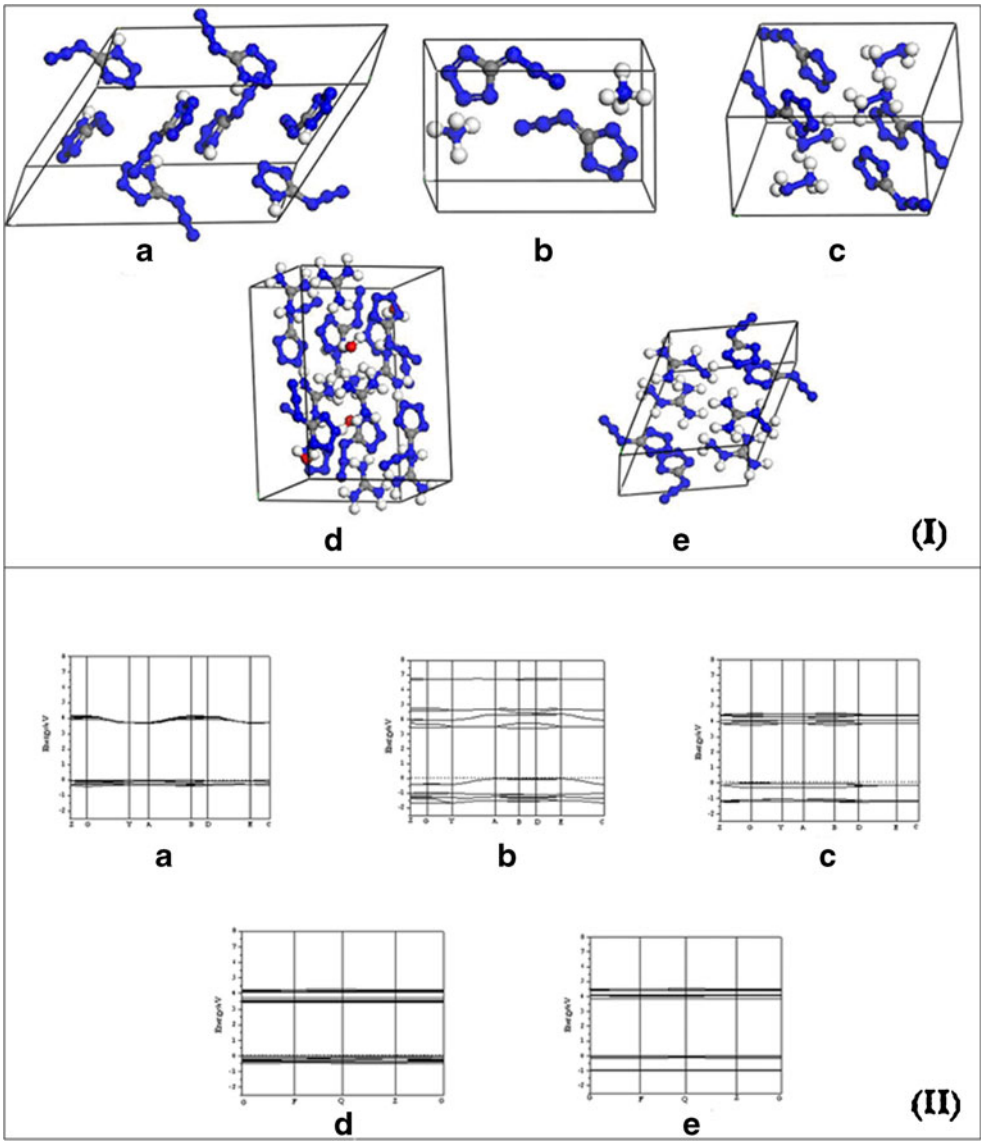

Fig. 1 (**I**) Schematic view of GGA-PW91 optimized the CN7 series crystal structures. **a** HCN_7, **b** $[NH_4]^+[CN_7]^-$, **c** $[N_2H_5]^+[CN_7]^-$, **d** $[CH_6N_3]^+[CN_7]^-\cdot H_2O$ and **e** $[CH_7N_4]^+[CN_7]^-$. *Blue* means nitrogen atom, *Gray* means carbon atom, and *white* means hydrogen atom. (**II**) Energy band structure of five compunds

Computational methods

The ground state properties of the title compounds based on the experience were calculated using a plane wave basis in the frame of density functional theory as implementented in the CASTEP code of Materials Studio 5.0 (MS 5.0) Program [20, 21]. We have used Vanderbilt-type ultrasoft pseudopotentials [22] to describe the electronion interactions. Band-by-band conjugated gradient method has been used to determine the self-consistent ground state of the system, while Pulay desity-mixing method was calculated for the electronic wave functions [23]. The structures were relaxed using the Broyden, Fletcher, Goldfarb, and Shannon (BFGS) method [24]. The exchange-correlation potential of Ceperley and Alder [25] as parametrized by Perdew and Zunger [26] in local density approximation (LDA) and also the generalized gradient approximation (GGA) with the Perdew-Burke-Ernzerhof (PBE) parametrization [27] was tried to describe the electron–electron interactions. From the comparation, GGA approximation has been confirmed for the system. A plane wave basis set with an energy cutoff of 340 eV has been used. For the Brillouin zone sampling, 2×5×2, 6×4×3, 2×3×3, 3×2×2 and 3×3×3 Monkhost-Pack

Table 1 Statistical assessment of the deviation between the calculated bond lengths (Å) and experimental ones for HCN_7[a]

Function	GGA		LDA	
	PW91	BP86	VWN	PWC
Δ_{max}	0.003	−0.267	−0.362	−0.360
MD	0.005	−0.110	−0.010	−0.009
MAD	0.012	0.011	0.019	0.019
RMS	0.014	0.015	0.021	0.021

[a] Δ_{max}, MD, MAD and RMS denote maximum, mean, mean absolute, and root mean square deviations, respectively

Table 2 Experimental and theoretical bond length Å^{-1} (the simulation results by using GGA-PW91 functions has been put in parentheses) of the series compounds

A				B		C	
N1-N2	1.355 (1.351)	N1′-N2′	1.352 (1.353)	N1-N2	1.358 (1.341)	N1-N2	1.348 (1.360)
N2-N3	1.295 (1.295)	N2′-N3′	1.293 (1.296)	N2-N3	1.306 (1.320)	N2-N3	1.317 (1.334)
N3-N4	1.372 (1.359)	N3′-N4′	1.369 (1.358)	N3-N4	1.360 (1.342)	N3-N4	1.352 (1.361)
N4-C1	1.321 (1.335)	N1′-C1′	1.33 (1.345)	N4-C1	1.337 (1.343)	N4-C1	1.327 (1.330)
N1-C1	1.327 (1.345)	N4′-C1′	1.32 (1.335)	N1-C1	1.316 (1.340)	N1-C1	1.330 (1.324)
N5-C1	1.383 (1.372)	N5′-C1′	1.386 (1.371)	N5-C1	1.402 (1.393)	N5-C1	1.410 (1.385)
N5-N6	1.267 (1.245)	N5′-N6′	1.263 (1.246)	N5-N6	1.250 (1.237)	N5-N6	1.252 (1.251)
N6-N7	1.117 (1.137)	N6′-N7′	1.119 (1.136)	N6-N7	1.125 (1.141)	N6-N7	1.123 (1.147)
						N8-N9	1.452 (1.469)
D				E			
N1-N2	1.350 (1.337)	N1′-N2′	1.354 (1.337)	N1-N2	1.354 (1.348)	N1′-N2′	1.356 (1.346)
N2-N3	1.309 (1.301)	N2′-N3′	1.306 (1.304)	N2-N3	1.299 (1.295)	N2′-N3′	1.308 (1.299)
N3-N4	1.359 (1.347)	N3′-N4′	1.364 (1.345)	N3-N4	1.347 (1.342)	N3′-N4′	1.349 (1.344)
N4-C1	1.333 (1.320)	N4′-C1′	1.335 (1.319)	N4-C1	1.329 (1.327)	N4′-C1′	1.331 (1.322)
N1-C1	1.319 (1.323)	N1′-C1′	1.313 (1.325)	N1-C1	1.319 (1.319)	N1′-C1′	1.310 (1.318)
N5-C1	1.406 (1.383)	N5′-C1′	1.393 (1.381)	N5-C1	1.403 (1.382)	N5′-C1′	1.412 (1.380)
N5-N6	1.254 (1.235)	N5′-N6′	1.260 (1.237)	N5-N6	1.246 (1.238)	N5′-N6′	1.250 (1.233)
N6-N7	1.128 (1.121)	N6′-N7′	1.124 (1.119)	N6-N7	1.103 (1.120)	N6′-N7′	1.120 (1.120)
N8-C2	1.330 (1.327)	N8′-C2′	1.318 (1.324)	N8-C2	1.325 (1.328)	N8′-C2′	1.315 (1.330)
N9-C2	1.330 (1.328)	N9′-C2′	1.326 (1.325)	N8-N9	1.408 (1.411)	N8′-N9′	1.397 (1.417)
N10-C2	1.304 (1.320)	N10′-C2′	1.317 (1.324)	N10-C2	1.323 (1.324)	N10′-C2′	1.315 (1.320)
O1-H1A	0.907 (0.969)			N11-C2	1.323 (1.323)	N11′-C2′	1.313 (1.324)
O1-H1B	0.858 (0.973)						

mesh [28] has been used for compound **A**~**E** respectively. The total energy of the system was converged in 1.0×10^{-5} eV, and the remaining forces on the atoms are less than 0.03 eV Å^{-1}. The displacement of atoms less than 0.001 Å, and the residual bulk stress less than 0.05 GPa. The smearing width was set as 0.05 eV to converge more easily. For the relaxed structures, the Mulliken charges and bond orders were studied by using B3LYP/6-311G(3d,2p) level in Gaussian 03 program [29, 30], and the Dmol^3 module of MS 5.0 has been used to analyze the relative thermodynamic properties from the results of the frequencies.

Before further calculation, two typical types (LDA and GGA) were applied to bulk HCN_7 as a test. Four methods including VWN [31], PWC [32] functionals of LDA type and BP86 [33, 34], PW91 [34, 35] functionals of GGA type have been compared to choose the most appropriate for the system. However, both GGA and LDA calculations show the structure parameters assigned by bond lengths are close to the experimental results. The differences of bond lengths between the simulation and the experiment are defined as r_{calc}-r_{exp}, the statistical analysis of the bond lengths is given in Table 1. According to the deviation values, the BP86, VWN and PWC functionals make bond lengths shorter than experiment data significantly, while PW91 functionals yield slightly longer bond lengths. Obviously, PW91 meta GGA functional

Table 3 Experimental and relaxed bond angles/° (the simulation results using GGA-PW91 functions is in parentheses) for title compounds

Bond Angle	A	B	C	D	E
N1-C1-N5	122.2 (121.)	126.7 (126.7)	121.9 (121.1)	125.3 (125.6)	127.6 (126.7)
N4-C1-N5	129.5 (129.7)	120.5 (120.5)	125.4 (124.9)	122.1 (119.6)	119.8 (121.1)
N1-C1-N4	108.3 (108.8)	112.8 (112.7)	112.5 (113.9)	112.6 (114.8)	112.6 (112.2)
C1-N1-N2	108.1 (107.7)	103.5 (102.5)	103.9 (103.3)	104.4 (102.3)	103.5 (104.4)
N1-N2-N3	107.1 (106.7)	110.3 (108.9)	109.6 (109.6)	109.5 (110.5)	110.5 (109.5)
C1-N5-N6	116.2 (114.1)	117.3 (117.8)	115.8 (113.7)	114.9 (116.1)	116.5 (115.1)
N5-N6-N7	171.7 (171.2)	171.6 (171.8)	171.6 (172.3)	173.2 (172.3)	172.2 (173.5)

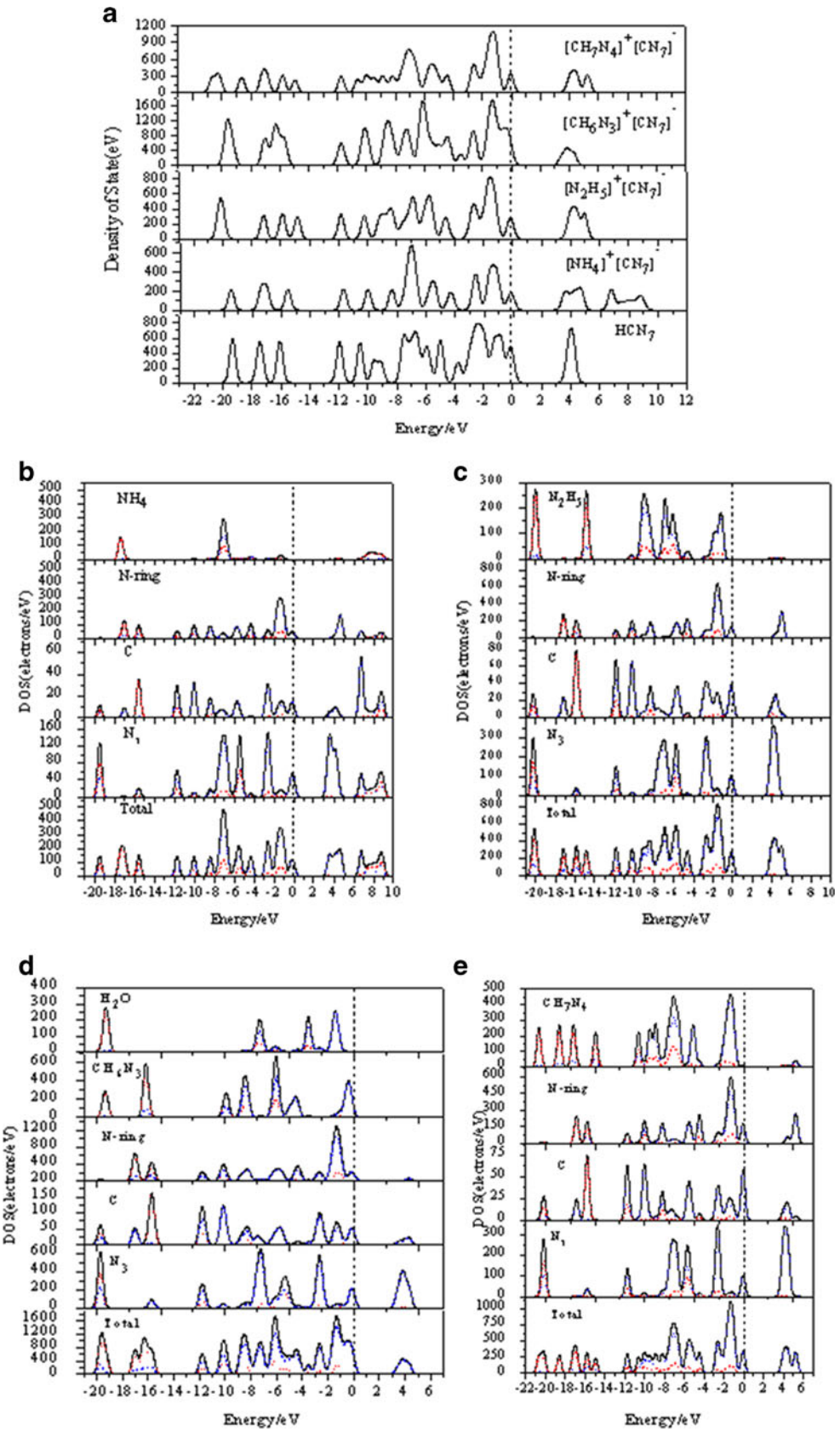

Fig. 2 **a** Total density of state (DOS) of the title compounds obtained by GGA-PW91 function. The Fermi energy is shown as *dashed vertical line*. **b**~**e** are the total and partial density of states (PDOS) of the four salts, respectively

Table 4 The calculated charge variation (eV) by using B3LYP/6–311G(3d,2p) level for crystalline **B**, **C**, **D** and **E**

Compound	B	C	D	E
Anion(CN_7^-)	−0.71	−0.79	−0.72	−0.72
Cation	0.71	0.79	0.72	0.72

performs best, which is in accordance with previous observations for the geometries of alkali metal azides [36]. In conclusion, the accuracy of the four tested functions for the inferred geometries is PW91>BP86>PWC>VWN. Thus in further study, the GGA (PW91) has been used for the other four compounds, which may be expected to gain more dependable predictions of the structure.

Results and discussion

Bulk structure

The optimized bond lengths and bond angles for the five structures are given in Tables 2 and 3 together with their experimental values [13]. The results of calculation agree with experiment very well. The N-N bond lengths of -N_3 (1.119~1.251 Å) are significantly shorter than those in tetrazole circle (1.295~1.361 Å). The N6-N7 is the shortest in the molecule, while the N5-C1 is the longest. It indicates the interaction between azido and tetrazole is relatively weak. Meanwhile, the length of N-N in azide (1.120 Å~1.246 Å) is similar to that in heavy-metal azides (1.141~1.212 Å), but longer than in alkali metal azides (1.171 ~1.176 Å) [36]. Also there is a distinction between azido-tetrazole and its salts: the bond lengths in tetrazole circle of the salts are longer than that in HCN_7. It can be concluded the combination of atoms become weaker when losing one hydrogen ion. For the bond angles, they are all around 108° in azido-tetrazole, but the penta-ring will distort when a hydrogen atom is lost.

Band energy and density of state

The electronic band structures of the five compounds were investigated by first-principle shown in Fig. 1(II). Seen from Fig. 1(II), the band structure of HCN_7 is analogous to the other four salts, in which the conduction band fluctuates significantly while the valence bands are relatively flat. However, there are several different typical features. Firstly, the results of **A**, **B**, **C**, **D** and **E** display large energy gaps of 3.968 eV, 3.407 eV, 3.882 eV, 3.425 eV and 3.522 eV between valence and conduction bands, respectively. The large band gaps indicate that there is nearly no conductivity in the azido-tetrazole salts. Generally, the wider band-gap is expected to be less energetic, while the smaller band-gap is opposite. This result agreed with the conclusion that **A** (5-azido-tetrazole) and its four salts are somewhat extremely high energetic compounds with increased sensitivities. Secondly, some bands crossed with each other among the band structures of **A** indicating its covalent nature, but the phenomenon is disappearing gradually in the four ion salts, even turning parallel in that of **E** compound. Thirdly, comparing the energy bands in the direction of reciprocal vector of Brillouin areas of the four ion salts, the variety of the frontier band curve with the k value is not apparent, demonstrating that the covalent interactions between electrons in valence orbit become weaker, which means they have obvious hole effective masses.

To obtain more information about the bond nature of azido-tetrazole, the electronic density of states (DOS) of its

Table 5 The bond order by using B3LYP/6–311G(3d,2p) level for **A**, **B**, **C**, **D** and **E**

A		B		C		D		E	
Bond	Bond order	Bond	Bond order	Bond	Bond order	Bond	Bond order	Bond	Bond order
N1-N2	0.71	N1-N2	0.79	N1-N2	0.80	N1-N2	0.80	N1-N2	0.77
N2-N3	0.91	N2-N3	0.83	N2-N3	0.84	N2-N3	0.87	N2-N3	0.88
N3-N4	0.75	N3-N4	0.79	N3-N4	0.81	N3-N4	0.78	N3-N4	0.79
N4-C1	1.02	N4-C1	0.97	N4-C1	1.02	N4-C1	1.01	N4-C1	0.98
N1-C1	0.94	N1-C1	1.00	N1-C1	1.00	N1-C1	1.02	N1-C1	1.02
N5-C1	0.83	N5-C1	0.75	N5-C1	0.76	N5-C1	0.76	N5-C1	0.77
N5-N6	0.95	N5-N6	0.98	N5-N6	0.98	N5-N6	0.98	N5-N6	0.97
N6-N7	1.41	N6-N7	1.38	N6-N7	1.41	N6-N7	1.42	N6-N7	1.42
				N8-N9	0.41	N8-C2	0.94	N8-C2	0.97
						N9-C2	0.94	N8-N9	0.54
						N10-C2	0.95	N10-C2	0.94
								N11-C2	0.95

salts were studied and shown in Fig. 2a. Several general characters can be observed. Although the peaks of DOS cross the Fermi energy levels (this is affected by the big smearing width value in the setting), the large band gaps of the five still indicate that they can hardly conduct electricity. Secondly, there are some similarities on the shape of the curve in DOS between **A** and its salts. That means these compounds have similar electronic properties. Furthermore, the energy-spans of the four salts are all larger than the initial compound **A**. The result showed the degeneration of the energy band of **D** is the largest because the covered area of the density of state is the smallest. For another aspect, the ionicity is increased as the sequence **B**<**C**<**D**<**E** because the energy-spans of valence bands are smaller and smaller.

The atom-resolved DOS and partial density of states (PDOS) of the four azido-tetrazole salts are displayed in Fig. 2 **b**~**e**. At the Fermi energy level, the DOS of the four crystals are limited because of the broadening effect. In the higher valence band, the peak near the Fermi level is sharp. Three obvious peaks for all of the structures appear in the top valence band region. These peaks are predominately consisted of the *p* states. Moreover, for the high valence some chief peaks are classified by the *s* and *p* states. The conduction band is dominated by the *p* states. It can be concluded that the *p* states play a very important role in their chemical reaction of the four solids.

The peaks of PDOS are dominated by the N-*p* state in the tetrazole rather than the azides at the Fermi leve. However, the electrons of valence in C atoms do not transit from −4.0 eV to Fermi level suggesting they play the role of an electron donor in the compound. Furthermore, the contributions of cation for DOS are increasing as the following sequence: **B**>**C**>**D**>**E**. In this aspect, the azido-tetrazole slats are not purely ionic systems.

Some sharp peaks in the PDOS of the C atoms and -N_3 group indicate they are in the same energy level, and the stable relashionship between C atom in tetrazole and -N_3. It is similar with N and C atoms in tetrazole. Some differences in the PDOS for the title compounds are due to the differences in their local molecular structure.

The peaks of the salts are dominated by the N_3-*p* states in the conduction band, while the contributions of N atoms in the tetrazole are relatively small. It is obvious that the high occupied orbital and low unoccupied orbital of the crystals is constituted by the *p* electronic -N_3 in azido-tetrazole. It can be inferred that -N_3 is the active part of the four compounds. The C-N_3 bonds may first be broken when suffering shear strain, impact wave, or distortion. The electrons in the azido will be excited to its empty orbit and then migrated to other electronic orbits. So we predicted the azido-tetrazole salts are sensitivity, which is already supported by experiment.

Charge variation and bond order

The atom charge variation (mainly the Mulliken charge) and the bond order have been investigated by using B3LYP/6-311G(3d,2p) level in Gaussian 03 to get the electronic structures of title compounds. The results have been listed in Tables 4 and 5. In compounds **B** and **C** (the positive charge is centered on the N atom in both of them), the charge of CN_7^- is decreased from −0.71 to −0.79 eV while the range is the same for the cation from 0.71 to 0.79 eV when the content of nitrogen increased. That means there will be two results for introducing energetic groups, it will increase the polarity of the salt when N^+ is the center, but there are no affects to the polarity for introducing –NH_2 in **D** and **E** where C^+ are their center. So **B** and **C** are more superior primary explosive materials for the higher sensitivity. For other aspects, the results demonstrate that these azido-tetrazole salts are inclined to perform covalence character, which is in agreement with the previous conclusions.

Bond order was calculated to analyze the strength between atoms. It is seen from Table 5 that the overlap between the N atoms at the end of –N_3 and that in the middle of –N_3 (N6-N7) is the highest (1.38~1.42); so it is the steadiest part of the series compounds. On the other hand, the bond strength of N atoms on the tetrazole (N1-N2) is the lowest in **A**, indicating it is the active part, which may first

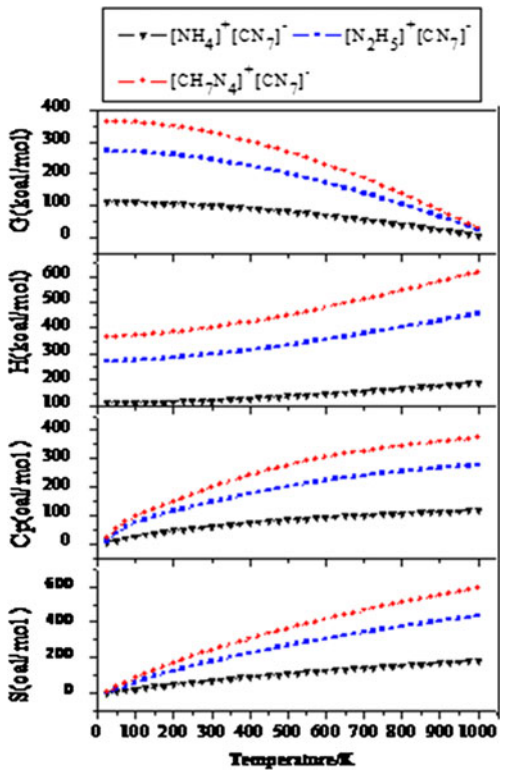

Fig. 3 The entropy, heat capacity, enthalpy and free energy variate with the increasing temperature of the series compounds. (The result was obtained by the the Dmol^3 module of MS 5.0 program)

crack when being stimulated. However, for **B** and **D** compounds, the weakest parts are between azido group and the tetrazole. Hence the dossociation or the explosive may be triggered by the loss of $-N_3$, and this is similar with the compounds **C** and **E**. The explosive mechanism is likely led by the loss of the azido group.

Thermodynamic properties

The contents of nitrogen of **B**, **C** and **E** are increased sequently, while D is an exception as one molar H_2O is contained in the crystal. Their entropy, heat capacity, enthalpy and free energy changes with different temperature were investigated by $Dmol^3$ module of Material Studio 5.0 program and summarized in Fig. 3. The entropy of the three crystals increases linearly with increasing temperature. That is because the translation and rotation of the molecule is the main performance in low temperature, which is a low-energy performance. While with the temperature increased, the main affect of entropy is the vibration of molecule that is a high-energy motion. So the entropy increased as the figure shows. The trend of the enthalpy and heat capacity is similar with the entropy except that of the Gibbs free energy. The sequence of the free energy is decreased as **E**>**C**>**B**. Obviously, the thermodynamic parameter is proportional to the nitrogen atoms in this series compound.

Conclusions

In this study, a comparative density functional theory in the generalized gradient approximation of the compound HCN_7 and its salts with high nitrogen contents was performed. The differences in the geometrical and electronic structures among these crystals have been investigated. The results of GGA-PW91 function are reasonable for the system.

The peaks of PDOS at Fermi level are dominated by the N-*p* states in the tetrazole ring, and the *p* electrons of azido play an important role. However, the peaks of the four salts in the conduction band are dominated by the N_3-*p* states. Considering the data from bond order, the $-N_3$ group combined with tetrazole circle is the active part of the compounds, which may decomposit first in thermal reaction. All of them are the latent energetic ligand of primary explosive, in which **B** and **C** appear better for their polarity bond properties. The explosive should be triggered by losing the azido group from the simulation.

Acknowledgments The financial support from the National Natural Science Foundation of China and China Academy of Engineering Physics (NSAF: 10776002), the Program for New Century Excellent Talents in University (NCET-09-0051), and the project of State Key Laboratory of Science and Technology (No. ZDKT12-03 & QNKT11-06) is gratefully acknowledged.

References

1. Thiele J, Marais JT (1893) Eur J Org Chem 273:144–160
2. Lesnikovieh AI, Levehik SV, Balabanovieh AI (1992) Thermochim Acta 200:427–444
3. Morisson H (1968) Chemistry of explosive derivatives of tetrazoles. Accession number: N69-13510, NTIS Issue Number: 6905
4. Kamlet MJ, Adolph HG (1979) Propellants Explor 4:30–34
5. Lieberman LM (1985) Ind Eng Chem Res 24:436–440
6. Lieberman ML, Fronabarger JW (1980) Status of the Development of 2-(5-Cyanotetrazolato) penta ammine cobalt (III) Perchlorate for DDT Devices. 7th Int Pyrotechnics Seminar, Vail, CO
7. Graeber EJ, Morosln B (1983) Acta Crystallogr C Cryst Struct Commun 39:567–570
8. Pickard JM (1984) J Hazard Mater 9:121–131
9. Hammerl A, Holl G, Klapötke TM et al. (2002) Eur J Inorg Chem 2002:834–845
10. Hammerl A, Klapötke TM, Nöth H et al. (2001) Inorg Chem 40:3570–3573
11. Hammerl A, Klapötke TM, Nöth H et al. (2003) Propell Explos Pyrotech 28:165–173
12. Hammerl A, Klapötke TM, Peter M et al. (2005) Propell Explos Pyrotech 30:17–26
13. Stierstorfer J, Klapötke TM, Hammerl A et al. (2008) Z Anorg Allg Chem 634:1051–1057
14. Hammer A, Hiskey M (2005) Chem Mater 17:3784–3793
15. Cao ZX, Xiao HM, Zhang SW (1999) J Mol Struct 46:167–173
16. Gao A, Oyumi Y, Brill TB (1991) Combust Flame 83:345–352
17. Stolle RG (1931) J Prakt Chem/Chem-Ztg 132:18
18. Hammerl A, Klapötke TM (2002) Inorg Chem 41:906–912
19. Denffer MV, Klapötke TM, Sabaté CM (2008) Z Anorg Allg Chem 634:2575–2582
20. Hohenberg P, Kohn W (1964) Phys Rev B 136:864
21. Segall MD, Lindan PJD, Probert MJ (2002) J Phys Condens Matter 14:2717–2744
22. Dolg M, Wedig U (1987) J Chem Phys 86:866–872
23. David V (1990) Phys Rev B 41:7892–7895
24. Fletcher R (1980) Practical methods of optimization. Wiley, New York
25. Ceperley DM, Alder BJ (1980) Phys Rev Lett 45:566–569
26. Perdew JP, Zunger A (1981) Phys Rev B 23:5048–5079
27. Perdew JP, Burke K, Ernzerhof M (1996) Phys Rev Lett 77:3865–3868
28. Monkhorst HJ, Pack JD (1976) Phys Rev B 13:5188–5192
29. Mulliken RS (1955) J Chem Phys 23:1833–1846
30. Frisch MJ, Trucks GW, Schlegel HB et al. (2004) Gaussian 03. Gaussian Inc, Pittsburgh
31. Vosko SH, Wilk L, Nusair M (1980) Can J Phys 58:1200–1206
32. Perdew JP, Wang Y (1992) Phys Rev B 45:13244–32248
33. Becke AD (1988) Phys Rev A 38:3098–3104
34. Perdew PJ (1986) Phys Rev B 33:8822–8824
35. Perdew PJ, Burke K, Wang Y (1996) Phys Rev B 54:16533–16539
36. Ogden JS, Dyke JM, Levason W et al. (2006) Chem Eur J 12:3580–3586